LAWRENCE
LIVERMORE
NATIONAL
LABORATORY

LLNL-JRNL-412676

ARM Climate Modeling Best Estimate Data

S. Xie, R. McCoy, S. Klein, R. Cederwall, W. Wiscombe, E. Clothiaux, K. Gaustad, J.-C. Golaz, S. Hall, M. Jensen, K. Johnson, Y. Lin, C. Long, J. Mather, R. McCord, S. McFarlane, G. Palanisamy, Y. Shi, D. Turner

May 1, 2009

Bulletin of the American Meteorological Society

Disclaimer

LLNL-JRNL-412676

ARM Climate Modeling Best Estimate Data

- A new data product for climate studies

S. Xie, R. B. McCoy, S. A. Klein, R. T. Cederwall, W. J. Wiscombe, E. E. Clothiaux, K. L. Gaustad, J.-C. Golaz, S. Hall, M. P. Jensen, K. L. Johnson, Y. Lin, C. N. Long, J. H. Mather, R. A. McCord, S. A. McFarlane, G. Palanisamy, Y. Shi, and D. D. Turner

Affiliations: *Xie, McCoy, Klein, Cederwall – Lawrence Livermore National Laboratory, Livermore, California; Hall, McCord, and Palanisamy – Oak Ridge National Laboratory, Oak Ridge, Tennessee; Clothiaux – The Pennsylvania State University, University Park, Pennsylvania; Gaustad, Long, Mather, McFarlane, Shi – Pacific Northwest National Laboratory, Richland, Washington; Golaz, Lin – NOAA Geophysical Fluid Dynamics Laboratory, Princeton, New Jersey; Jensen, Johnson, Wiscombe – Brookhaven National Laboratory, Upton, New York; Turner – University of Wisconsin-Madison, Madison, Wisconsin.*

Corresponding author: *Shaocheng Xie, Atmospheric, Earth and Energy Division (L-103), Lawrence Livermore National Laboratory, P.O. Box 808 Livermore, CA 94550.*

E-mail: xie2@llnl.gov

Submitted to *BAMS* on 11May 2009

Revised on 19 September 2009

Category: *NOWCAST*

Section: *Product Announcement*

1. Introduction

The U.S. Department of Energy (DOE) Atmospheric Radiation Measurement (ARM) Program (www.arm.gov) was created in 1989 to address scientific uncertainties related to global climate change, with a focus on the crucial role of clouds and their influence on the transfer of radiation in the atmosphere. A central activity is the acquisition of detailed observations of clouds and radiation, as well as related atmospheric variables for climate model evaluation and improvement. Since 1992, ARM has established six permanent ARM Climate Research Facility (ACRF) sites and deployed an ARM Mobile Facility (AMF) in diverse climate regimes around the world (Fig. 1) to perform long-term continuous field measurements. The time record of ACRF data now exceeds a decade at most ACRF fixed sites and ranges from several months to one year for AMF deployments. Billions of measurements are currently stored in millions of data files in the ACRF Data Archive.

The long-term continuous ACRF data provide invaluable information to improve our understanding of the interaction between clouds and radiation and an observational basis for model validation and improvement and climate studies. Given the huge number of data files and current diversity of archived ACRF data structures, however, it can be difficult for an outside user such as a climate modeler to quickly find the ACRF data product(s) that best meets their research needs. The required geophysical quantities may exist in multiple data streams, and over the history of ACRF operations the measurements could be obtained by a variety of instruments, be reviewed with different levels of data quality assurance, or derived using different algorithms. In addition, most ACRF data are stored in daily-based files with a temporal resolution that ranges from a few seconds to a few minutes, which is much finer than that sought by some users.

Therefore, it is not as convenient for data users to perform quick comparisons over large spans of data, and this can hamper the use of ACRF data by the climate community.

To make ACRF data better serve the needs of climate studies and model development, ARM has developed a data product specifically tailored for use by the climate community. The new data product, named the Climate Modeling Best Estimate (CMBE) dataset, assembles those quantities that are both well observed by ACRF over many years and are often used in model evaluation into one single dataset. The CMBE product consists of hourly averages and thus has temporal resolution comparable to a typical resolution used in climate model output. It also includes standard deviations within the averaged hour and quality control flags for the selected quantities to indicate the temporal variability and data quality. Since its initial release in February 2008, the new data product has quickly drawn the attention of the climate modeling community. It is being used for model evaluation by two major U.S. climate modeling centers, the National Center for Atmospheric Research (NCAR) and the Geophysical Fluid Dynamics Laboratory (GFDL).

The purpose of this paper is to provide an overview of CMBE data and a few examples that demonstrate the potential value of CMBE data for climate modeling and in studies of cloud processes and climate variability and change.

2. CMBE dataset overview

The current CMBE dataset contains 11 cloud and radiation relevant quantities, such as the cloud fraction, cloud liquid water path, and surface radiative fluxes, from long-term ARM measurements (Table 1). These quantities are measured by a set of ACRF ground-based active and passive remote sensing instruments, including Millimeter-Wavelength Cloud Radars

(MMCRs), Micropulse Lidars (MPLs), laser ceilometers, Microwave Radiometers (MWRs), Solar and Infrared Radiation Stations (SIRSs), and Total Sky Imagers (TSIs). Through its Value-Added Product (VAP) efforts (Peppler et al. 2008), ARM has implemented advanced retrieval algorithms and sophisticated objective data analysis approaches to process and integrate data collected from these instruments. The outputs of these efforts are geophysical quantities that represent the most accurate estimate possible of clouds and their microphysical and radiative properties. Most quantities in CMBE are assembled from four VAPs, including the Active Remote Sensing of CLouds (ARSCL, Clothiaux et al. 2000) VAP which provides the best estimate of the vertical location of clouds by integrating measurements from MMCR, MPL, and laser ceilometers, the Microwave Radiometer Retrievals (MWRRET, Turner et al. 2007) VAP which uses an advanced retrieval algorithm to derive cloud liquid water path and column precipitable water from MWR measurements, and the Data Quality Assessment for ARM Radiation Data (QCRAD, Long and Shi 2006, 2008) VAP for surface radiative fluxes. To further improve CMBE data, we apply additional quality control checks, such as outlier and time variability checks. More details can be found from the CMBE Web page (http://science.arm.gov/wg/cpm/scm/best_estimate.html).

CMBE data are currently available for the Southern Great Plains (SGP) Lamont site, the North Slope of Alaska (NSA) Barrow site, and the Tropical Western Pacific (TWP) Manus, Nauru, and Darwin sites (Table 2). CMBE data can be obtained from the ACRF data archive (http://iop.archive.arm.gov/arm-iop/0showcase-data/cmbe/). Statistical views of all CMBE products can be found from the ARM Archive's Statistical Browser interface (http://www.archive.arm.gov).

3. Potential applications

Field data are often used in studies of atmospheric processes. As the time record of ARM program data increases, CMBE data can also be used to examine climate variability and change, as well as to statistically evaluate climate models. Below we provide a few examples illustrating these purposes.

a. Process studies

Process studies are important tools used to increase our scientific understanding of cloud systems and provide new ideas that may lead to improved cloud parameterizations. The CMBE dataset provides a variety of observational cases in different climate regimes to support such studies. The hourly time resolution and high vertical resolution support detailed examination of vertical structures and temporal evolution of the selected cloud systems and their macrophysical and radiative properties. Figure 2 provides an integrated example of how clouds and their properties evolve as a summer storm develops from shallow cumulus convection to deep convection during one day at SGP. The detailed observations of clouds and radiation provide invaluable information to understand the structure and temporal variability of the observed cloud system and assist cloud parameterization improvements.

b. Diurnal and seasonal cycles

Diurnal and seasonal cycles are two fundamental modes of climate variability. Because cloud radars and lidars in space are on satellites that poorly sample the diurnal cycle, ground-based radars and lidars are the primary source of information on the diurnal cycle of cloud vertical structure. Therefore, the long-term CMBE dataset of ground-based measurements provides a

distinct opportunity to examine the vertical distribution of clouds on diurnal and seasonal timescales.

Figure 3a shows a composite of the diurnal cycle of clouds in the summer months (June, July, and August) at SGP. CMBE data display the prominent maximum in upper tropospheric clouds due to nocturnal precipitation, as well as the occurrence of shallow cumulus clouds that grow atop the daytime boundary layer. The distinct features in diurnal variations of different types of clouds pose a great challenge for climate models. As illustrated in Figure 3b, current climate models have difficulties in correctly capturing some of the observed features in diurnal variations. The GFDL Atmospheric Model version 2 (AM2) (GFDL Global Atmospheric Model Development Team 2004) is unable to reproduce the development of shallow cumulus clouds during the day. Similar model error is also found in the NCAR Community Atmosphere Model version 3. The correct representation of the diurnal variability of clouds in climate models is important for accurate calculation of radiative fluxes. For example, the absence of shallow clouds in AM2 may partly explain its overestimate of shortwave radiation reaching the surface, which in turn leads to a large warm 2-meter temperature bias over that area in AM2 climate simulations (not shown). This model-observation comparison provides key information that could focus parameterization improvement efforts.

Clouds also exhibit large geographical and seasonal variability. Figure 4 shows the seasonal variation in monthly mean clouds at the five ACRF sites. As revealed by the CMBE dataset, cloud vertical extents are greater at the tropical sites and lower at the polar site reflecting variations in depth of the troposphere. At the SGP site, the maximum cloud occurrence is during the winter and spring months when high cirrus and low boundary layer clouds are predominant. There are relatively few clouds during the summer months or at middle levels between 2 km and

5 km. In contrast, low clouds are the major cloud type observed at the NSA Barrow site with the peaks occurring during late summer and early autumn. The TWP Manus site is located at the heart of the western Pacific warm pool. Cloud occurrence over Manus shows clear seasonal variation associated with the seasonal migration of the intertropical convergence zone and is much larger than that observed at the TWP Nauru site, which is situated on the eastern edge of the western Pacific warm pool where convection is usually less pronounced than that at Manus. Clouds over Darwin are mainly influenced by the northern Australian summer monsoon activity, therefore exhibiting a strong seasonal variability. Significant amounts of middle and high level clouds are observed during the monsoon season from December through March while only a few clouds at high and low levels are seen in other months, which represent the dry season over the Darwin region.

c. Arctic climate change

The Arctic is undergoing a rapid climate change towards a much warmer climate with significantly reduced sea-ice extent in the summer season. Changes in solar radiation may accelerate this warming through the ice-albedo feedback with cloud changes possibly playing a role. While global climate change due to greenhouse gases may be the ultimate driver of reduced sea ice, much of the year-to-year variability in sea-ice loss is associated with circulation fluctuations that help drive sea-ice loss. In particular, when high pressure is strong in the western Arctic Ocean, sea-ice loss is greater as shown in Ogi et al (2008). High pressure conditions bring significantly reduced cloud cover and increased downward solar radiation that, along with changes in surface wind stress, may contribute to the reduced sea-ice. CMBE data at Barrow show that anomalies in summertime high pressure are well correlated with downward solar

radiation anomalies for the last decade (Figure 5). This suggests that observations at Barrow may be useful in monitoring changes in western Arctic climate in general and clouds and radiation in particular.

d. Decadal brightening over land

Recent studies have shown that surface downwelling solar radiation has undergone significant decadal variations over land surfaces. From the later 1990s to the 2000s, there is evidence of significant decadal increase of solar radiation reaching the Earth's surface, the so-called decadal "brightening". Significant decadal brightening is also shown in the long-term ARM radiation data record for both all-sky and clear-sky radiation (Figure 6). As demonstrated by Long et al. (2009), ARM surface solar radiation data along with other relevant measurements at SGP can be used to assess decadal brightening and to understand whether aerosols, clouds, or other factors are responsible for these changes.

4. Summary and future work

The primary purpose of developing a long-term, integrated best estimate dataset is to encourage greater use of ACRF data by the climate community. The dataset also allows the ACRF to generate statistical summaries of its high quality products. The CMBE product will be updated frequently in order to include the most recent observations. Furthermore, future releases of CMBE-related datasets will also include additional ACRF data such as atmospheric thermodynamic profiles, surface turbulent fluxes, conventional surface meteorological fields, soil measurements, radiative fluxes at top of the atmosphere, the vertical profile of cloud and aerosol properties, and radiative heating rates. Large-scale forcing for case studies with single-column

models and cloud-resolving models and area-mean quantities will be included also in the CMBE dataset for the ARM SGP and Darwin sites. Additionally, CMBE data will be developed for ACRF Mobile Facility deployments. Finally, monthly mean and monthly mean diurnal cycle climatologies derived from CMBE data will be released in the near future.

Acknowledgments. This project is supported by the DOE ARM program. Work at LLNL was performed under the auspices of the U. S. Department of Energy, Office of Science, Office of Biological and Environmental Research by Lawrence Livermore National Laboratory under contract No. DE-AC52-07NA27344. Recognition is also extended to those responsible for the operation and maintenance of the instruments that produced the data featured in this paper; their diligent and dedicated efforts are often underappreciated.

For future reading

Ackerman, T. P., and G. M. Stokes, 2003: The Atmospheric Radiation Measurement Program. *Phys. Today*, **56**, 38-44.

Clothiaux, E. E., T. P. Ackerman, G. G. Mace, K. P. Moran, R. T. Marchand, M. Miller, and B. E. Martner, 2000: Objective determination of cloud heights and radar reflectivities using a combination of active remote sensors at the ARM CART sites. *J. Appl. Meteor.*, ***39***, 645-665.

The GFDL Global Atmospheric Model Development Team, 2004: The new GFDL global atmosphere and land model AM2-LM2: Evaluation with prescribed SST simulations. *J. Climate*, ***17***, 4641-4673.

Kassianov, E., C. N. Long, and M. Ovtchinnikov, 2004: Cloud Sky Cover versus Cloud Fraction: Whole-Sky Simulations and Observations. *J. Appl. Meteor*., **44**, 86-98.

Long, C. N., J. M. Sabburg, J. Calbo, and D. Pages, 2006: Retrieving Cloud Characteristics from Ground-based Daytime Color All-sky Images. *Journal of Atmospheric and Oceanic Technology*, **23**, No. 5, 633–652.

Long, C. N. and Y. Shi, 2006: The QCRad Value Added Product: Surface Radiation Measurement Quality Control Testing, Including Climatologically Configurable Limits. *Atmospheric Radiation Measurement Program Technical Report*, ARM TR-074, **69** pp. Available via http://www.arm.gov/publications/tech_reports/arm-tr-074.pdf.

Long, C. N., and Y. Shi, 2008: An Automated Quality Assessment and Control Algorithm for Surface Radiation Measurements. *The Open Atmos. Sci. J*., **2**, 23-37, doi: 10.2174/1874282300802010023.

Long C. N., E. G. Dutton, J. A. Augustine, W. Wiscombe, M. Wild, S. A. McFarlane, and C. J. Flynn, 2009: Significant Decadal Brightening of Downwelling Shortwave in the Continental US. *J. Geophys. Res*., **114**, D00D06, doi:10.1029/2008JD011263.

Kay J. E., T. L'Ecuyer, A. Gettelman, G. Stephens, C. O'Dell, 2008: The contribution of cloud and radiation anomalies to the 2007 Arctic sea ice extent minimum. *Geophys. Res. Lett*., **35**, L08503, doi:10.1029/2008GL033451.

Ogi M., I. G. Rigor, M. G. McPhee, J. M. Wallace, 2008: Summer retreat of Arctic sea ice: Role of summer winds. *Geophys. Res. Lett*., **35**, L24701, doi:10.1029/2008GL035672.

Peppler, R.A. and coauthors, 2008: An overview of ARM program climate research facility data quality assurance. *The Open Atmos. Sci. J*., **2**, 192-216, doi:10.2174/1874282300802010192.

Turner, D.D., S.A. Clough, J.C. Liljegren, E.E. Clothiaux, K. Cady-Pereira, and K.L. Gaustad, 2007: Retrieving liquid water path and precipitable water vapor from Atmospheric Radiation Measurement (ARM) microwave radiometers. *IEEE Trans. Geosci. Remote Sens*., **45**, 3680-3690, doi:10.1109/TGRS.2007.903703.

Wild, M., H. Gilgen, A. Roesch, A. Ohmura, C. N. Long, E. G. Dutton, B. Forgan, A. Kallis, V. Russak, and A. Tsvetkov, 2005: From dimming to brightening: Decadal changes in solar radiation at the Earth's surface. *Science*, **308**, Issue 5732, 847-850. Doi: 10.1126/science. 1103215.

Wild, M., J. Grieser, and C. Schar, 2008: Combined surface solar brightening and increasing greenhouse effect support recent intensification of the global land-based hydrological cycle. *Geophys. Res. Lett*., **35**, L17706, doi:10.1029/2008GL034842.

Zhang, Y. and S. A. Klein, 2009: Mechanisms affecting transition from shallow to deep convection over land: Inferences from observations collected at the ARM Southern Great Plains site. *To be submitted to the Journal of Atmospheric Sciences.*

Figure Captions

Figure 1. Locations of ARM Climate Research Facility (ACRF) sites (Courtesy of U. S. Department of Energy's Atmospheric Radiation Measurement Program).

Figure 2. Vertical structure and temporal evolution of a cloud system observed on 17 June 2007 at SGP and its associated cloud and radiative properties: (a) cloud fraction, (b) cloud liquid water path (LWP), (c) precipitable water (PW), (d) surface downwelling shortwave radiative flux (SWDN), and (e) surface downwelling longwave radiative flux (LWDN).

Figure 3. Observed and modeled diurnal cycle of cloud fraction during the summer months (June, July, and August) from at SGP: (a) CMBE cloud fraction (1996-2007) and (b) GFDL AM2 cloud fraction (climatology).

Figure 4. Seasonal cycle of cloud fraction at the five ACRF sites: (a) SGP-Lamont, (b) NSA-Barrow, (c) TWP-Manus, (d) TWP-Nauru and (e) TWP-Darwin. Missing data are masked (black).

Figure 5. Time series of July-August-September (JAS) averaged sea-level pressure (SLP) index from Ogi et al. (2008) and downward shortwave radiation (SWDN) at Barrow from the CMBE dataset. The sea-level pressure index tracks the strength of the Western Arctic Ocean anti-cyclone that is very well correlated with sea-ice extent. Higher values of the index indicate higher pressure, more downward shortwave radiation, and less sea-ice extent.

Figure 6. Yearly averages of all-sky (blue) and clear-sky (red) downwelling shortwave (SWDN) (solid lines) over the period of 1996 – 2007 at the SGP Lamont site, along with their corresponding least-squares linear fits (dashed lines). (The figure was taken from Long et al., 2009.) In both cases downwelling shortwave irradiance shows a clear tendency of

increase over the study years, with the all-sky SW trend (6.1 Wm^{-2}/decade) being about twice that of the clear-sky increase (2.9 Wm^{-2}/decade).

Tables

Table 1. Geophysical quantities included in the current CMBE dataset

Quantity	Source	Instrument	Resolution in source files
Cloud fraction*	ARSCL (Clothiaux et al. 2000)	Cloud radar, lidar, and laser ceilometers	10s
Total cloud cover (narrow fields-of- view)	ARSCL	Cloud radar, lidar, and laser ceilometers	10s
Total cloud cover (wide fields-of-view)	TSI (Kassianov et al., 2004; Long et al., 2006)	Total sky imager	30s
Cloud liquid water path	MWRRET (Turner et al. 2007)	Microwave Radiometers	~ 25s
Precipitable water	MWRRET	Microwave Radiometers	~ 25s
Surface shortwave direct normal	QCRAD (Long and Shi, 2006, 2008)	Pyrheliometer	1min
Surface shortwave diffuse	QCRAD	Pyranometer	1min
Surface downwelling shortwave flux	QCRAD	Pyranometer	1min
Surface upwelling shortwave flux	QCRAD	Pyranometer	1min
Surface downwelling longwave flux	QCRAD	Pyrgeometer	1min
Surface upwelling longwave flux	QCRAD	Pyrgeometer	1min

*: Cloud fraction has a vertical resolution of 45 m in both source files and CMBE.

Table 2. CMBE data availability

ARM Site	Location	Available period
SGP-Lamont	97.5^0 W, 36.6^0 N	1996 - 2007
NSA-Barrow	156.6^0 W, 71.3^0 N	1998 - 2007
TWP-Manus	147.4^0 E, 2^0 S	1996 - 2007
TWP-Nauru	166.9^0 E, 0.5^0 S	1998 - 2007
TWP-Darwin	130.9^0 E, 12.4^0 S	2002 - 2007

Figures

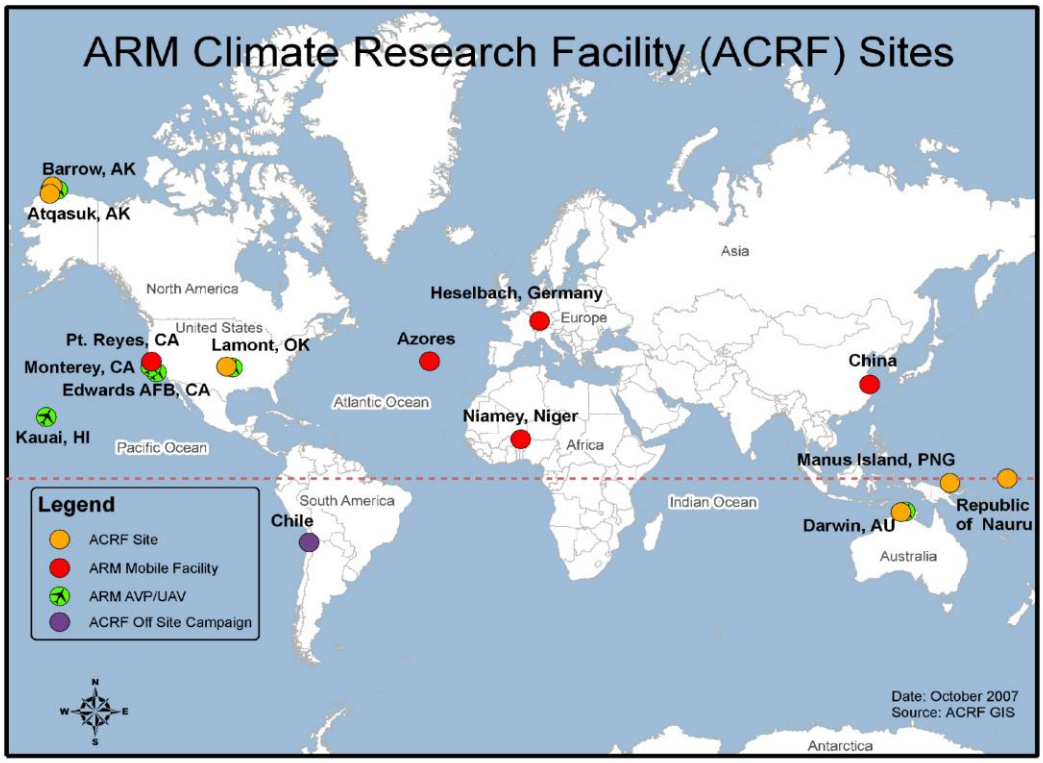

Figure 1. Locations of ARM Climate Research Facility (ACRF) sites (Courtesy of U. S. Department of Energy's Atmospheric Radiation Measurement Program).

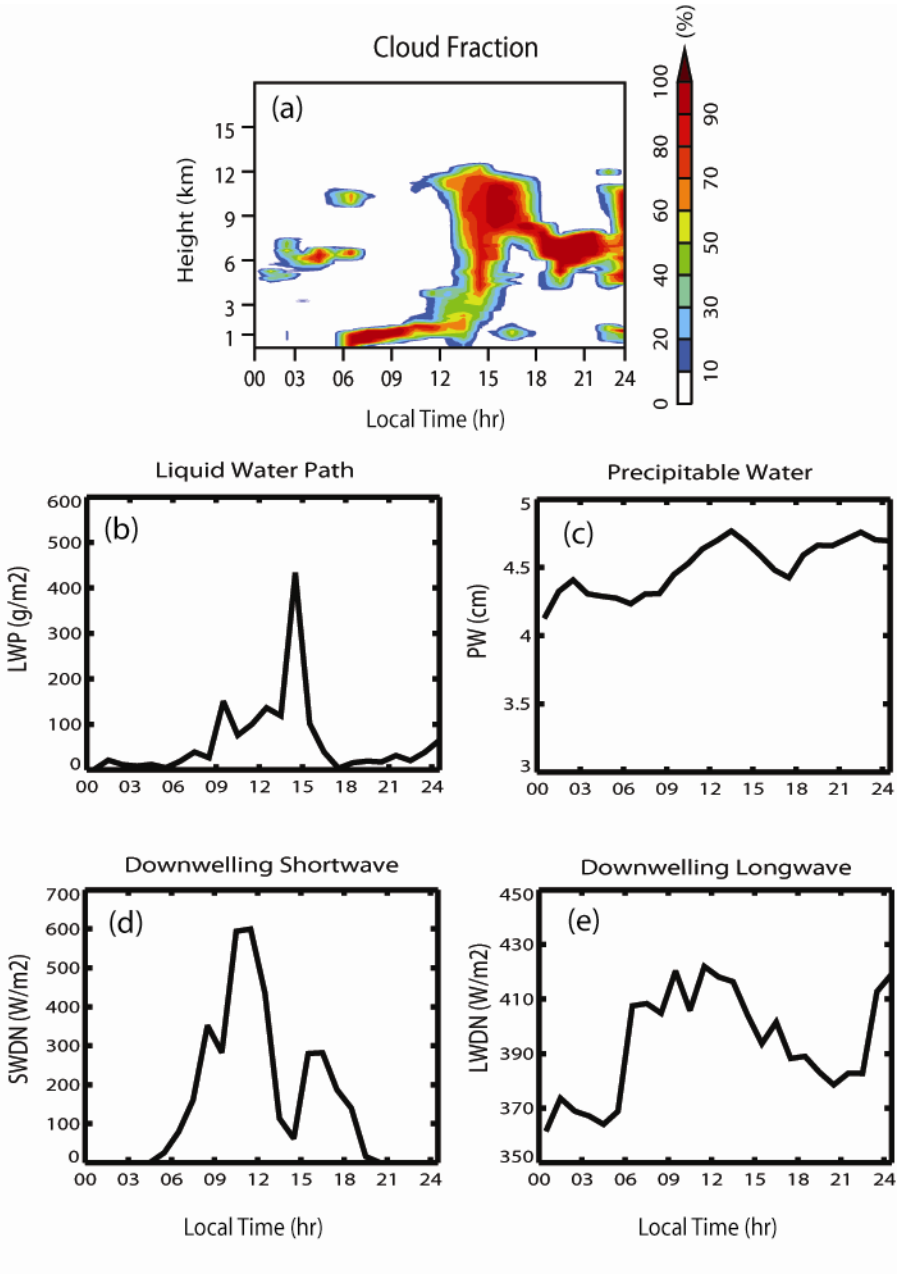

Figure 2. Vertical structure and temporal evolution of a cloud system observed on 17 June 2007 at SGP and its associated cloud and radiative properties: (a) cloud fraction, (b) cloud liquid water path (LWP), (c) precipitable water (PW), (d) surface downwelling shortwave radiative flux (SWDN), and (e) surface downwelling longwave radiative flux (LWDN).

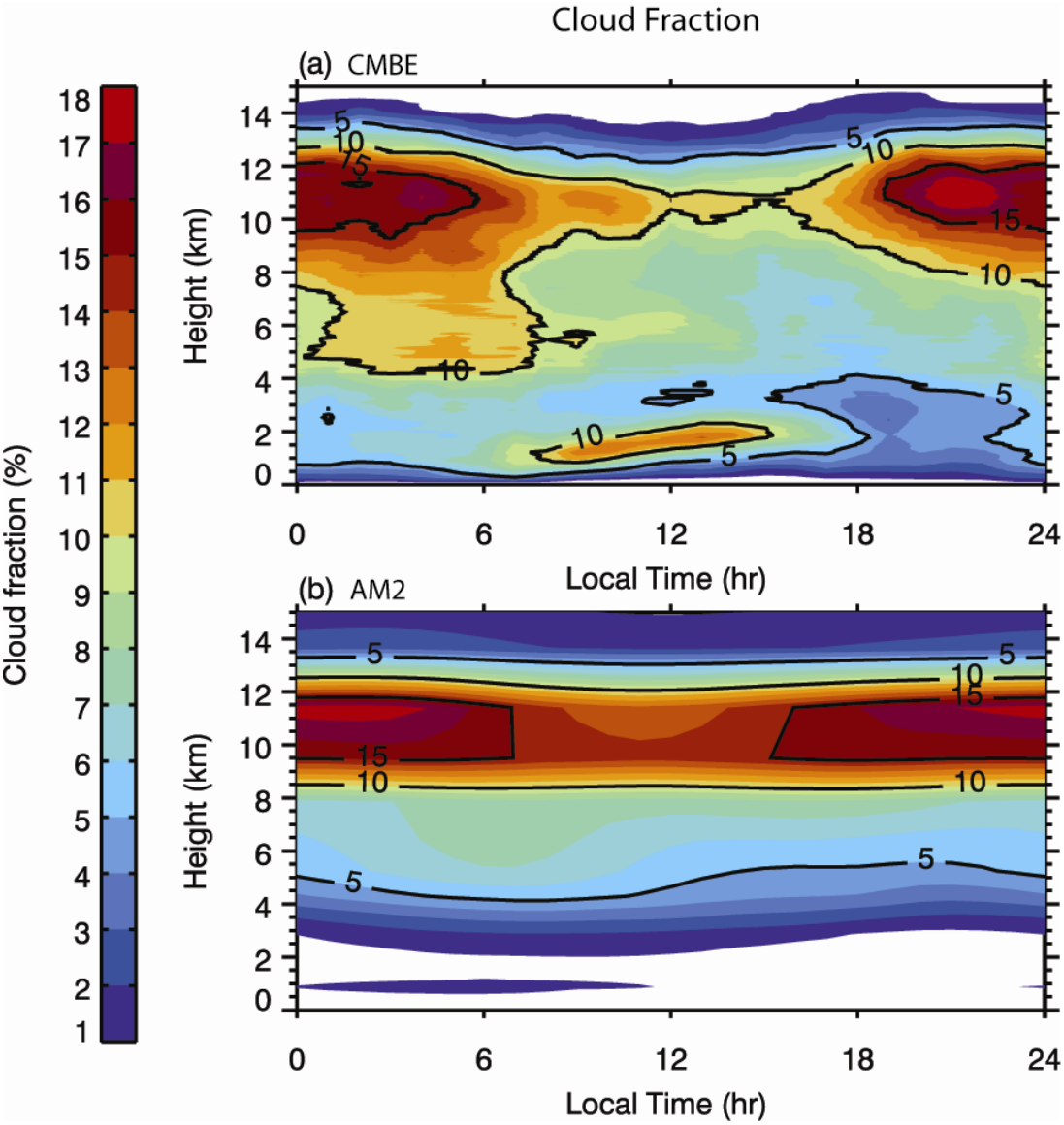

Figure 3. Observed and modeled diurnal cycle of cloud fraction during the summer months (June, July, and August) from at SGP: (a) CMBE cloud fraction (1996-2007) and (b) GFDL AM2 cloud fraction (climatology).

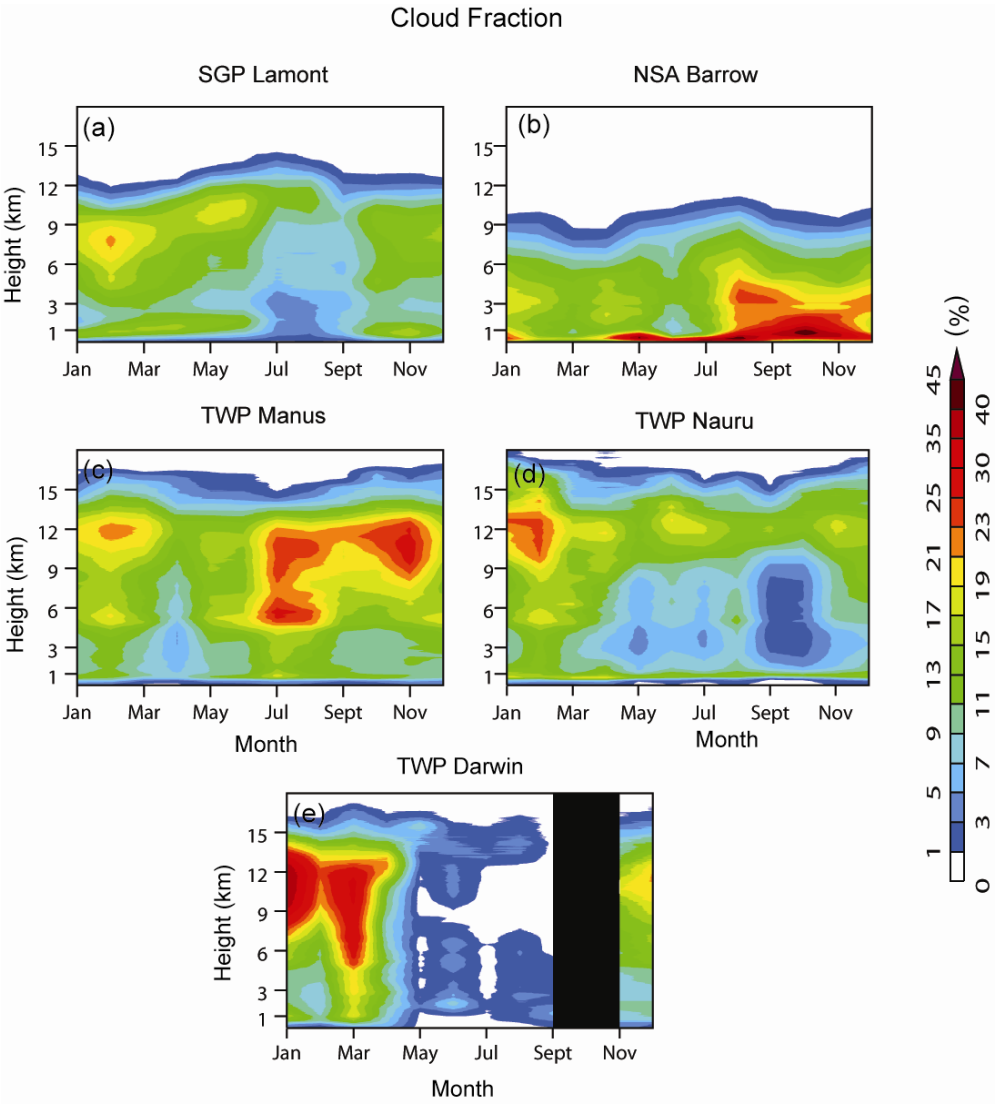

Figure 4. Seasonal cycle of cloud fraction at the five ACRF sites: (a) SGP-Lamont, (b) NSA-Barrow, (c) TWP-Manus, (d) TWP-Nauru and (e) TWP-Darwin. Missing data are masked (black).

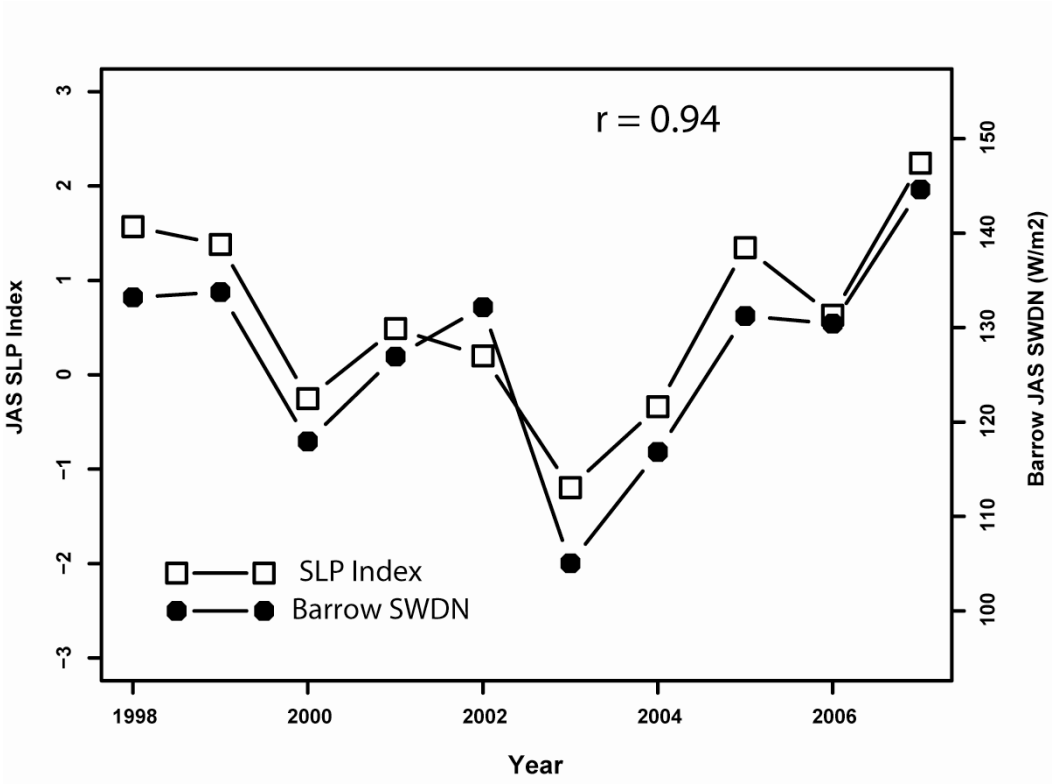

Figure 5. Time series of July-August-September (JAS) averaged sea-level pressure (SLP) index from Ogi et al. (2008) and downward shortwave radiation (SWDN) at Barrow from the CMBE dataset. The sea-level pressure index tracks the strength of the Western Arctic Ocean anti-cyclone that is very well correlated with sea-ice extent. Higher values of the index indicate higher pressure, more downward shortwave radiation, and less sea-ice extent.

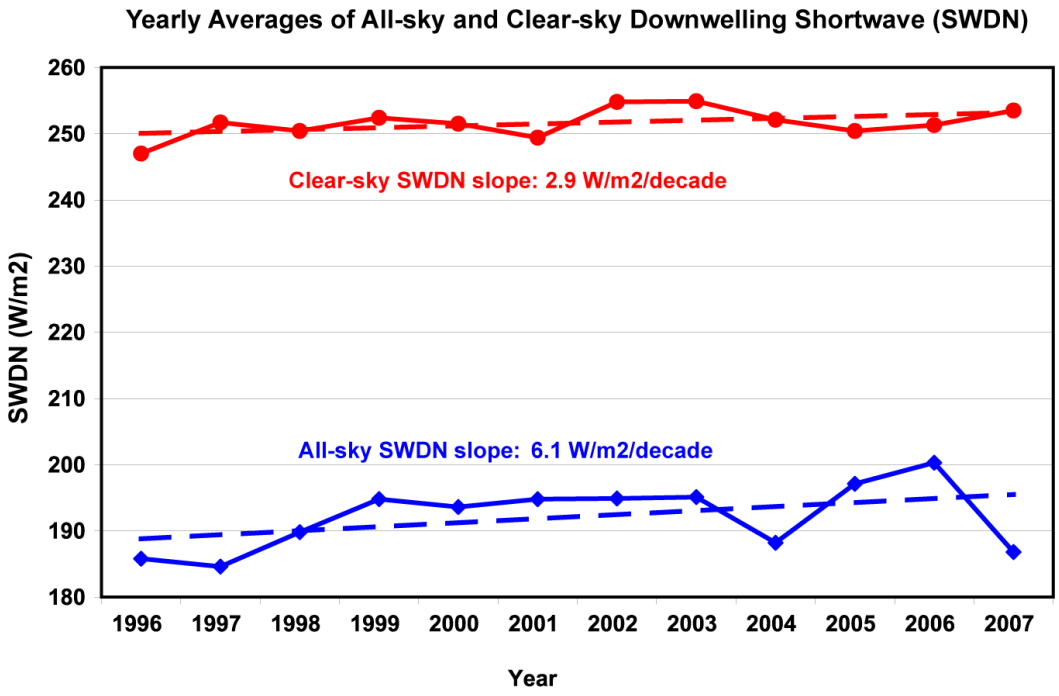

Figure 6. Yearly averages of all-sky (blue) and clear-sky (red) downwelling shortwave (SWDN) (solid lines) over the period of 1996 – 2007 at the SGP Lamont site, along with their corresponding least-squares linear fits (dashed lines). (The figure was taken from Long et al., 2009.) In both cases downwelling shortwave irradiance shows a clear tendency of increase over the study years, with the all-sky SW trend (6.1 Wm^{-2}/decade) being about twice that of the clear-sky increase (2.9 Wm^{-2}/decade).